Oxygen Vacancy Formation, Mobility, and Hydrogen Pick-up during Oxidation of Zirconium by Water

Citation for the original published paper (version of record):
Lindgren, M., Panas, I. (2017). Oxygen Vacancy Formation, Mobility, and Hydrogen Pick-up during Oxidation of Zirconium by Water. Oxidation of Metals, 87(3-4): 355-365.
http://dx.doi.org/10.1007/s11085-016-9695-z

Oxid Met (2017) 87:355–365
DOI 10.1007/s11085-016-9695-z

ORIGINAL PAPER

Oxygen Vacancy Formation, Mobility, and Hydrogen Pick-up during Oxidation of Zirconium by Water

Mikaela Lindgren[1] · **Itai Panas**[1]

Received: 21 December 2016 / Published online: 4 January 2017

Abstract A comprehensive first principles understanding of the oxidation of zirconium alloys by water was reiterated. Two channels were taken to jointly constitute to the oxidation process: one according to classical oxidation theory involving hydrogen evolution and the second reflected by inwards transport of protons causing hydrogen pick-up. The two were associated with charged and uncharged oxygen vacancies, respectively. The purpose of the present study was to clarify the nature of the effective anode during oxidation of zirconium as to the detailed role of the metal. Oxygen dissolution in the alloy resulted in a "pre-anodic" property associated with the formation of oxygen vacancy V_O in the oxide, i.e., preceding $V_O^{2+}/2e^-$ separation. Atomistic perspective on the metal/oxide interface before nucleation of V_O was provided. The rapid convergence of the model interface to bulk properties in spite of the local structural variability provided new insight as to the nature of an amorphous metal/oxide interface.

Keywords Zirconium oxidation · Anode process · Oxygen mobility · Theory from first principles

Introduction

The rate of any chemical reaction involving two and more reactants relies on their encountering. In addition, if the sources of the reactants are a priori separated in space, the reaction rate becomes controlled by the transport properties of the

✉ Mikaela Lindgren
mikaela.lindgren@chalmers.se

Itai Panas
itai.panas@chalmers.se

[1] Department of Chemistry and Chemical Engineering, Chalmers University of Technology, 412 96 Gothenburg, Sweden

interface between the sources. The very build-up of reaction product at this interface complicates further encounter between reactants. The protection of structural alloys from corrosion when being exposed to oxidizing conditions relies on the corresponding build-up of a durable oxide scale. Rather than being static, this scale is maintained by its growth, its ability to heal, as well as its ability to dominate the competing degradation processes. Competing processes may include scale dissolution at the metal/oxide interface, pore and crack formation in the oxide, scale re-crystallization, and even evaporation. Somewhat paradoxically, the increasing impacts of the said competing processes are indeed heralded by the ideal parabolic or sub-parabolic growth of the barrier oxide itself. This is because of the slow-down in the rate of growth owing to a decreasing chemical potential gradient. The thermodynamic drive for product formation is represented by the chemical potential difference between the two interfaces. While the driving force for the corrosion process reflects a generic thickness dependence of the chemical potential gradient, the rate of the oxide growth is determined in addition by the mobility of reactants through the barrier oxide.

At steady state, the net reaction during oxide growth is simply represented by metal and oxygen forming metal oxide. Typically, the oxide grows at the inner and outer interfaces, i.e., between metal and oxide and between oxide and corrosive environment, respectively. Often, channels for product formation involve vacancy creation at the interfaces, their migration thorough the oxide scale, and their annihilation at the opposite interfaces. Thus, oxygen vacancies formed at the metal/oxide interface diffuse through the oxide scale and become annihilated at the interface between oxide and oxidizing environment. Equivalently, metal vacancies form at the environment/oxide interface, diffuse through the oxide scale, and become annihilated at the interface between oxide and metal. Mobility of neutral such vacancies is seldom high. Instead, separation into mobile electrons and charged vacancies becomes an efficient way to maintain the oxide growth. This channel for oxide growth is captured by Wagner theory [1–4]. The annihilation of mobile entities may be separated in time causing a steady-state separation of charge, which in turn may impact the oxide growth itself, i.e., space charge effects. In what follows, inwards oxide growth is considered. It becomes tempting to designate anodic properties to the oxygen vacancy V_O generation at the metal/oxide interface owing to subsequent dissociation into to V_O^{2+} and $2e^-$. Correspondingly, the interface between oxide and oxidizing surrounding would take the role of cathode, e.g., due to oxygen reduction by $\frac{1}{2}\ O_2 + 2e^- \rightarrow O^{2-}$ or water reduction $H_2O + 2e^- \rightarrow O^{2-} + H_2$ preceding the annihilation of the charged vacancy by $V_O^{2+} + O^{2-} \rightarrow O_O$, i.e., the external oxygen ion occupying the charged oxygen vacancy.

Owing to its industrial importance, detailed understanding of zirconium oxidation by water has been acquired from first principles. Rather than atomistic simulation, the purpose of this effort was to build understanding by deconstructing the corrosion phenomenon into computationally accessible and at the same time experimentally relevant quantum chemical modules describing sub-processes relevant to anode [5, 6], cathode [6–8], and transport properties [9]. In autoclave, cyclic episodes of sub-parabolic oxide growth and subsequent breakdown of the

protective zirconia is observed on Zr-base alloys [10, 11]. In [9], we proposed that this breakdown is caused by a particular dissolution process whereby oxygen, a priori residing in the oxide scale, is dissolved in the Zr matrix. Breakdown occurs when the rates of migration and annihilation of oxygen vacancies generated at the metal/oxide interface become slower than the said dissolution process.

The purpose of the present study is to clarify further the nature of the effective anode during oxidation of zirconium as to the role of the metal. The objective is indeed to separate the conducting electrons in the alloy from the actual anodic property of the metal/oxide interface. A "pre-anodic" property of the oxygen vacancy is arrived at, preceding the $V_O^{2+}/2e^-$ separation.

Computational Details

Conceptual insight is sought by means of first principles calculations using density functional theory (DFT) [12, 13]. The CASTEP program package [14] within the Material Studios framework [15] was utilized and the PBE GGA functional [16] was employed for all calculations. Core electrons were described by ultrasoft pseudopotentials [17] in conjunction with 340 eV cut-off energy.

The present study utilizes a periodically repeating interface between t-ZrO_2 and α-Zr, while to some extent ambiguous, it was designed to satisfy approximate epitaxy by matching the 100 plane of t-ZrO_2 to the 010 plane of α-Zr. The resulting supercell, consisting of 120 atoms, was geometry optimized including optimization of the lattice parameters, see Fig. 1. The lattice parameters were held constant in the subsequent calculations. The *k*-point sampling of the Brillouin zone was made by means of the Monkhorst–Pack scheme [18] with a $2 \times 2 \times 1$ *k*-points mesh. Neutral oxygen vacancies were created by moving one oxygen atom from the oxide to an interstitial position in the α-Zr matrix. The lattice parameters were kept constant in order to determine lower bounds to the oxygen dissolution. The vacancy positions are indicated in Fig. 1. The interstitial oxygen in the Zr matrix is positioned at the interface in order to capture the instantaneous local drive for dissolution. Bulk properties are reported elsewhere [5]. The complete linear synchronous transit/quadratic synchronous transit (LST/QST) method [19] was employed to estimate transition states for oxygen vacancy diffusion. The reference calculations on bulk t-ZrO_2 were done on a supercell with 48 atoms.

Result and Discussion

A useful definition of an anodic site is that this is where oxidation takes place. However, owing to the requirement of electro-neutrality of chemical reactions, any oxidation process must be associated with a reduction reaction. Here, though, we address microscopic processes at the nominal anode. In doing so, properties preceding the actual oxidation reaction are addressed.

This study concerns particular aspects of the continued oxidation process of zirconium alloys by water. The process is known to display inwards oxide growth.

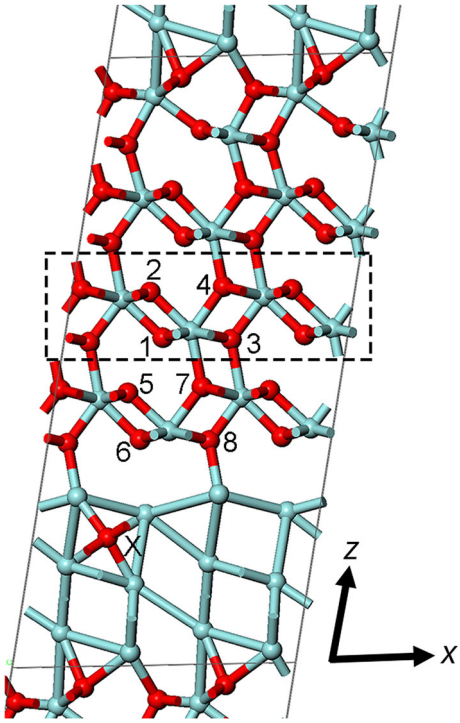

Fig. 1 Supercell model [20] of metal/oxide interface on which calculations were performed. The positions where an oxygen vacancy was created in the comparative study are indicated with 1–8. The oxygen atom in the metal is indicated with *X*. *Red balls* refer to oxygen and *light blue* to zirconium. Lattice parameters of the box are $a = 11.03$ Å, $b = 6.89$ Å, $c = 24.02$ Å, $\alpha = 90.0°$, $\beta = 79.8°$, $\gamma = 88.7°$

Here, this is taken to imply initial oxygen vacancy creation at the metal/oxide interface. This process is driven by the high solubility of oxygen in zirconium, i.e., ~30 at% O [6, 21]. Crucial is the distinction between neutral and oxidized oxygen vacancies, i.e., V_O and V_O^{2+}, respectively. The former is present prior to oxidation. It results from zirconium alloy dissolving only neutral oxygen atoms. By doing so, oxygen nominally oxidizes the metal, while the metal ions at the oxide site where the oxygen emanated from are reduced. The latter is because the remaining electrons initially associated with the oxygen atom are forced to stay in the oxide. We say that V_O formation offers a preparatory step in the forming of the actual anode. This is in contrast to the anodic process which involves the dissociation of V_O into V_O^{2+} and $2e^-$.

In what follows, a representative model interface between metal and oxide is validated. In paragraph III.a, the relevance of the model is justified by the small energies associated with the formation of the V_O sites upon transferring a lattice oxygen into an interstitial site in the Zr matrix. In paragraph III.b, the band structure in bulk zirconia is mapped onto the local density of states in the oxide scale. In paragraph III.c, electronic signatures and mobility of an oxygen vacancy in bulk zirconia are reproduced by the interface. In section "Emerging Understanding", the results are put in context of a novel theory for oxidation of zirconium by water.

Energetics for Oxygen Vacancy Formation

The thermodynamically preferred dissolution of ZrO_2 in Zr is taken here to result from inter-diffusion of oxygen atoms into interstitial sites in the Zr alloy as accompanied by the corresponding formation of oxygen vacancies in the zirconia. The enthalpy of formation of a neutral oxygen vacancy (V_O) in the oxide at a metal/oxide interface by incorporating oxygen at interstitial site in the Zr matrix, for the various oxygen origins indicated in Fig. 1, is listed in Table 1.

While there are local variations, in particular the immediate interface clearly expresses the chemical incompatibility of the two phases. When comparing for example sites 6 and 8, the terminal role of the former as compared to the integrated position of the latter is taken to explain the increased stability on dissolution of O at site 6. It is interesting however, that already less than 1 nm into the oxide, the drive for dissolution stabilizes, *cf.* sites 1–4. The corresponding enthalpies of formation of neutral vacancies in bulk come out endothermic by approximately 0.5 eV in the periodic supercell calculations for both the tetragonal and monoclinic phases [9]. This articulates both similarity and dissimilarity of thermodynamic phases and the corrosion process, i.e., emphasizing the impact of proximity. This is further emphasized by the electronic signatures as reflected in the build-up of the band gap including impurity state owing to oxygen vacancy, in the oxide adjacent to the metal/oxide interface, vide infra.

Oxygen Vacancy Formation at Metal/Oxide Interface

The deconvolution of the total density of state (DOS) into its separate local metal and local oxide contributions is provided in Fig. 2a, b.

By comparing the latter contribution to that of the DOS in bulk ZrO_2, it is striking to note how rapidly convergence is achieved. A further manifestation of the similarity of bulk ZrO_2 electronic properties to the oxide at less than 1 nm from the metal/oxide interface is obtained by considering the characteristics of the oxygen vacancy, *cf.* Figure 2b, c. Indeed, also the position of the vacancy band in the local band gap reproduces that is observed in bulk, see Fig. 2 again. Looking closer into the decomposition of the total DOS at the interface and the Fermi energy (E_F) of the metal part, it is tempting to ascribe the metal as an infinite source of electrons, and

Table 1 Enthalpies of formation of oxygen vacancy at the metal/oxide interface, created by transfer to an interstitial site in the metal, see Fig. 1

Oxygen vacancy position	Enthalpy of formation [eV]
1	−0.29
2	−0.33
3	−0.08
4	−0.03
5	−0.69
6	−1.26
7	−0.37
8	−0.61

Negative values refer to exothermic processes

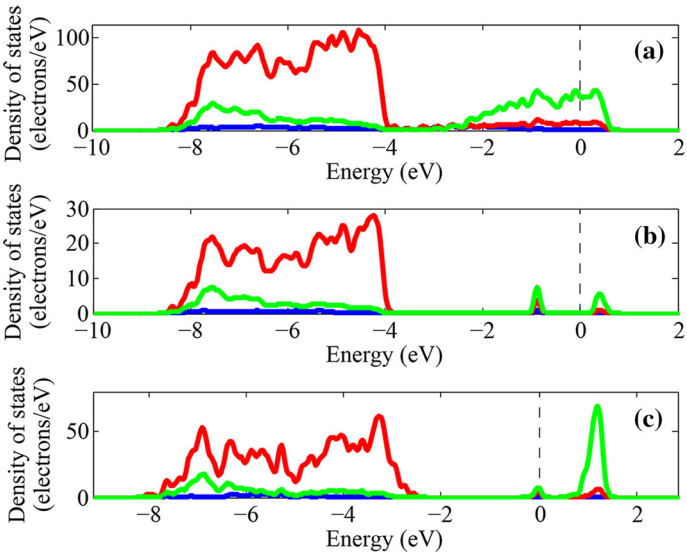

Fig. 2 **a** Density of states (DOS) for metal and oxide when an oxygen vacancy is created at position 1, see Fig. 1. **b** Oxide contribution to DOS, *dashed rectangle* in Fig. 1. The state associated with the oxygen vacancy is found ~1 eV below the Fermi energy (*dashed*) rendering it neutral. **c** DOS of t-$ZrO_{2-\delta}$ bulk, containing 3.1 at% O vacancies for comparison. *Blue* represents O 2s states, *red* O 2p states, and *green* Zr 4d states

in particular so as the V_O state lays below the E_F of the metal. It may be erroneously inferred that V_O is always replenished with electrons upon oxidation, owing to the cathode processes. This is however not the case, as it would imply net charging of the metal. This was understood by Wagner. It is argued here that a better way to understand the role of the metal, is it acting oxygen sink. The electrons of the V_O site become accessible to the cathode process by dissociating from the said site and diffusing in a background of equivalent V_O^{2+} sites. This implies a steady state build-up of space charge determined by the diffusion of V_O^{2+} to the cathode where they become annihilated by external O^{2-} ions, i.e., the products of the reduction process at the nominal cathode. This is discussed further in section "Emerging Understanding".

Oxygen Vacancy Mobility

The activation energy for oxygen vacancy V_O diffusion is associated with the rising and setting of the vacancy band on passing the transition state. Again, semi-quantitative agreement between a property at metal/oxide interface and that of bulk ZrO_2 is found. This finding puts to rest hypotheses based on spontaneous transient charging of the vacancy as a predominant means to lower the transition state, i.e., by transient injection of vacancy electrons into the conduction band of the metal. Rather, such easy paths should be deemed relevant only at low coverages. Indeed, the activation energy (E_A) for oxygen diffusion in bulk was found to depend

sensitively on the occupation of the VO band. Thus, activation energies of neutral V_O sites came out in vicinity of 2 eV and charged sites display $E_A < 0.5$ eV [9]. Thus, the energetics serve to further support the consistency in the comparison between local oxide properties metal/oxide interface (see Table 2) and those of ZrO_2 bulk.

Emerging Understanding

Here, we summarize our comprehensive understanding [5–9] and put the present findings in III.a–c in that context. In autoclave studies on water oxidation of zirconium alloys, cyclic episodes of sub-parabolic oxide growth and subsequent breakdown of the protective zirconia are observed. In [9], it was indeed proposed that this breakdown is caused by a particular dissolution process whereby oxygen, a priori residing in the oxide scale, is dissolved in the Zr matrix. This was explicitly addressed in paragraphs III.a–c. The breakdown of the barrier oxide is taken to initiate when the rates of migration and annihilation of oxygen vacancies generated at the metal/oxide interface becomes slower than the said dissolution process. Two channels were found to contribute to the oxidation process, one according to classical oxidation theory involving hydrogen evolution at the effective cathode (see Fig. 3), and one which allows inwards transport of protons against the electric field, i.e., hydrogen pick-up. The two channels were associated with charged V_O^{2+} and uncharged oxygen vacancy V_O formations at the metal/oxide interface. The first channel, i.e., classical oxidation theory, is summarized in Fig. 3. The sub-division of oxide layers into t-ZrO_2 at metal oxide interface in conjunction with an outer m-ZrO_2 is inspired by the study by Garner et al. [22]. Consistency of this understanding is provided in [9] based on transport properties of oxygen vacancies.

The barrier oxide of zirconia is taken to be subdivided into a defect-rich tetragonal phase providing both electron and ion conductivity, and a defect-free monoclinic phase permeating water in the form of hydroxides resulting from the hydrolysis products of O^{2-} and H_2O. The cathode process, occurring at the interface between tetragonal and monoclinic phases, comprised hydrogen evolution in conjunction with annihilation of charged oxygen vacancies in the tetragonal phase. The oxygen vacancies is formed by the dissolution process of oxygen in the Zr alloy, and their transient charging is the result of the defective tetragonal phase offering pathways for electron tunneling connecting preexisting charged oxygen vacancies. The diffusion of charged oxygen vacancies is similarly associated with very small activation energies.

Table 2 Effect of vicinity to metal on the activation energy (E_A) for vacancy diffusion

Path 1 E_A [eV]	Path 2 E_A [eV]	Path 3 E_A [eV]
1 → 2: 1.9	1 → 3: 2.5	2 → 4: 2.7
6 → 5: 1.8	6 → 8: 1.9	5 → 7: 2.0

Three different paths are presented with the distances 2.530, 2.699, and 2.860 Å for path 1, path 2, and path 3, respectively. The vacancy positions are indicated in Fig. 1a

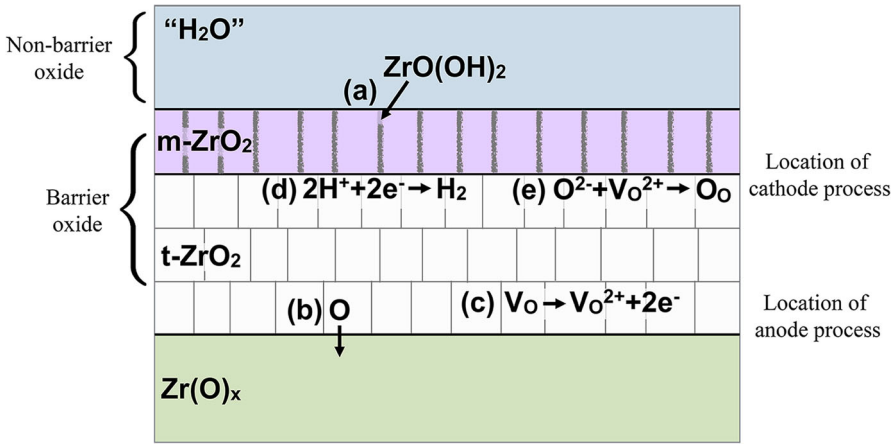

Fig. 3 **a** Hydroxylation of m-ZrO_2 grain boundaries at m-ZrO_2/"H_2O" interface. **b** The formation of neutral vacancies by oxygen dissolution in α-Zr at the t-ZrO_2/metal interface. **c** Charging of oxygen vacancies, i.e., anode reaction. **d** Hydrogen evolution at m-ZrO_2/t-ZrO_2 interface, i.e., cathode reaction. **e** Annihilation of charged oxygen vacancies at m-ZrO_2/t-ZrO_2 interface

From the formalism developed in [9], we have a thickness-dependent activation energy for diffusion owing to a constant bulk contribution and that originates from charging. The effective diffusivity of oxygen vacancies of charge q $D^q_{\text{eff}}(X)$ given by

$$D^q_{\text{eff}}(X) = D^q_{\text{bulk}} \exp\left[-\frac{q^2 C^{q+}_{V_O}}{8\varepsilon\varepsilon_0 k_B T} X^2\right], \tag{1}$$

where X is the oxide thickness, D^q_{bulk} is the diffusivity constant for vacancy of charge q in bulk, $C^{q+}_{V_O}$ is the concentration of charged oxygen vacancies, ε is the relative permittivity, ε_0 is the vacuum permittivity, k_B is Boltzmann constant, and T is the temperature. Given a constant concentration of charged oxygen vacancies, the activation energy increase for the formation of transient charged oxygen vacancies has a quadratic thickness dependence. From Eq. 1, a sub-parabolic oxide thickness curve was derived,

$$X = \left\{\lambda_q^2 \ln\left(1 + \frac{2K^q_p}{\lambda_q^2} t\right)\right\}^{\frac{1}{2}} \tag{2}$$

where t is time, $\Delta\mu$ is electro-chemical potential,

$$K^q_p = D^q_{\text{bulk}} \frac{\Delta\mu}{k_B T} \tag{3}$$

and

$$\lambda_q^2 = \frac{8\varepsilon\varepsilon_0}{q^2 C_{V_O^{q+}}} k_B T. \quad (4)$$

The total activation energy W for transport of oxygen vacancies by utilizing channels, which propagate electrons and charged vacancies separately, becomes

$$W = W_{\text{bulk}}^q + \frac{k_B T}{\lambda_q^2} X^2. \quad (5)$$

The first term in Eq. 5 represents the activation energy for bulk diffusion, while the second term is the thickness-dependent activation energy. It is associated with the forming charged vacancies. This second term causes sub-parabolic oxide growth in classical Wagnerian oxidation theory with H_2 evolution. In case of W_{bulk}^q large, the thickness-dependent term will not impact the scale growth. If on the other hand W_{bulk}^q is small, then the sub-parabolic behavior will dominate the mass gain curve. Relevant here is that charged oxygen vacancies in t-ZrO_2 display $\sim$0.2 eV activation energies for diffusion, i.e., five times smaller than those for uncharged vacancies. Equation 5 says that for constant density of charged vacancies, the cost for the formation of additional charged vacancies increases with thickness of barrier oxide to the power of two. The hydrogen pick-up channel opens owing to the slowing down of the Wagnerian channel, which in turn precedes the transition to the next cycle. We propose that the charging of the oxide causes the build-up of V_O concentration close to the metal/oxide interface owing to the dissolution of oxygen into the alloy. A symptom of the oxide dissolution process is neutral oxygen vacancies accumulation, super-saturation, and possible hydrogen-assisted nucleation late in each cycle. The formation of pores was taken to offer easy paths for short-circuiting hydrogen transport through the oxide [9, 23], resulting in the avalanching hydrogen pick-up [24] reported to precede the breakdown of the barrier oxide, the latter resulting from increased loss of mechanical integrity of the barrier oxide.

Conclusions

It was inferred in [9] that the rapid sudden increase in hydrogen pick-up fraction (HPUF) on approaching transition [24, 25] is associated with the formation of pores that build from the metal/oxide interface. Thus, the avalanche in hydrogen pick-up fraction was taken to reflect such pore formation, a symptom rather than the cause of barrier oxide breakdown. This study contributes the local atomistic perspective on the pre-nucleation of neutral oxygen vacancies at the metal/oxide interface. The drive to dissolve oxygen in the alloy is reflected in the results. Moreover, the rapid convergence of electronic properties to those of bulk oxide less than 1 nm into the oxide in spite of the local structural variability provides new insight as to the nature of an amorphous metal/oxide interface. New light is shed on the anode process during metal oxidation. Rather than the metal acting electron source, oxygen

dissolution in the alloy matrix produces oxygen vacancies V_O. Connection to Wagner theory is made if these become local anodes, i.e., by dissociating into $V_O^{q+} + qe^-$. The role of V_O^{q+} is dual. Displaying enhanced mobility relative to V_O, the presence of charged oxygen vacancies at steady state offers percolation pathways to the cathode by consecutive electron tunneling processes. This understanding of zirconia formers serves a conceptual platform including also alumina formers [26, 27].

Acknowledgements The Swedish Research Council, Westinghouse Electric Sweden AB, Sandvik Materials Technology AB, Vattenfall AB, and the EPRI (Electric Power Research Institute) are gratefully acknowledged for financial support.

References

1. C. Wagner, *Progress in Solid State Chemistry* **10**, 3 (1975).
2. C. Wagner, *Z Physics and Chemistry B* **21**, 25 (1933).
3. C. Wagner, *Atom Movements*, (American Society of Metals, Cleveland, Ohio, 1951), pp. 153–173.
4. P. Kofstad, *"Growth of Oxide Scales by Lattice Transport" in High temperature corrosion*, (Elsevier Applied Science Publishers LTD, Essex, England, 1988), p. 162.
5. M. Lindgren and I. Panas, *RSC Advances* **4**, 11050 (2014).
6. M. Lindgren, G. Sundell, I. Panas, L. Hallstadius, M. Thuvander and H.O. Andrén, Toward a comprehensive mechanistic understanding of hydrogen uptake in zirconium alloys by combining atom probe analysis with electronic structure calculations, (ASTM Special Technical Publication STP1543, West Conshohocken, 2015), pp. 515–539.
7. M. Lindgren and I. Panas, *RSC Advances* **3**, 21613 (2013).
8. M. Lindgren and I. Panas, *Beilstein Journal of Nanotechnology* **5**, 195 (2014).
9. M. Lindgren, C. Geers and I. Panas, Oxidation of Zr Alloys by Water—Theory from First Principles, Submitted to *Corrosion Science*, (2016).
10. E. Hillner, D. G. Franklin and J. D. Smee, *Journal of Nuclear Materials* **278**, 334 (2000).
11. B. Cox, *Journal of Nuclear Materials* **336**, 331 (2005).
12. P. Hohenberg and W. Kohn, *Physical Review B* **136**, B864 (1964).
13. W. Kohn and L. J. Sham, *Physical Review* **140**, A1133 (1965).
14. S. J. Clark, M. D. Segall, C. J. Pickard, P. J. Hasnip, M. J. Probert, K. Refson and M. C. Payne, *Zeitschrift Fur Kristallographie* **220**, 567 (2005).
15. Materials Studio 6.0, Accelrys Software Inc. (2011).
16. J. P. Perdew, K. Burke and M. Ernzerhof, *Physical Review Letters* **77**, 3865 (1996).
17. D. Vanderbilt, *Physical Review B* **41**, 7892 (1990).
18. H. J. Monkhorst and J. D. Pack, *Physical Review B* **13**, 5188 (1976).
19. N. Govind, M. Petersen, G. Fitzgerald, D. King-Smith and J. Andzelm, *Computational Materials Science* **28**, 250 (2003).
20. To obtain a 3-dimensional visualization of the model, contact mikaela.lindgren@chalmers.se.
21. J. P. Abriata, J. Garcés and R. Versaci, *Bulletin of Alloy Phase Diagrams* **7**, 116 (1986).
22. A. Garner, A. Gholinia, P. Frankel, M. Gass, I. MacLaren and M. Preuss, *Acta Materialia* **80**, 159 (2014).
23. M. Lindgren, C. Geers and I. Panas, Possible origin and roles of nano-porosity in ZrO_2 scales for hydrogen pick-up in Zr alloys, submitted to *Journal of Nuclear Materials* (2016).
24. A. Couet, A. T. Motta and R. J. Comstock, *Journal of Nuclear Materials* **451**, 1 (2014).

25. M. Harada and R. Wakamatsu, in *"The Effect of Hydrogen on the Transition Behavior of the Corrosion Rate of Zirconium Alloys" in Zirconium in the Nuclear Industry: 15th International Symposium*, eds. B. Kammenzind and M. Limback (ASTM, West Conshohocken, 2009), pp. 384–402.
26. M. Y. Yang, K. Kamiya, B. Magyari-Köpe, M. Niwa, Y. Nishi and K. Shiraishi, *Applied Physics Letters* **103**, 093504 (2013).
27. V. Babic, C. Geers, M. Lindgren, B. Jönsson, L-.G. Johansson, J-.E. Svensson, I. Panas,"Effects on Oxygen Vacancy Diffusivity of Substitutional 3d Elements Doping in alpha-Alumina" Submitted to *Oxidation of Metals*, 9th International Symposium on High-Temperature Corrosion and Protection of Materials (2016).